

Thermal stability of a binary non-faceted/non-faceted peritectic organic alloy at elevated temperatures

J.P. Mogeritsch,* A. Ludwig, S. Eck, M. Grasser and B.J. McKay

University of Leoben, Department of Metallurgy, Franz-Josef Str. 18, 8700 Leoben, Austria

Received 11 December 2008; revised 30 January 2009; accepted 30 January 2009

Available online 5 February 2009

The organic substances NPG (neopentylglycol) and TRIS (tris(hydroxymethyl)aminoethane) are known to show a non-faceted/non-faceted peritectic phase diagram. The present investigation compares direct observations of the organic peritectic alloy made in a Bridgman furnace and differential scanning calorimetry measurements with the reported phase diagram. Investigations of the long-term stability showed decomposition tendencies depending on concentration and applied temperatures. Nevertheless, a process window is suggested which can be used for directional solidification experiments under stable conditions.

© 2009 Acta Materialia Inc. Published by Elsevier Ltd. All rights reserved.

Keywords: Peritectic solidification; Thermal analysis; Organic model alloy

A number of transparent organic substances and their alloys have been investigated to find model substances that allow an in situ and real-time observation of metal-like solidification phenomena such as dendritic, cellular or eutectic growth morphologies [1–6]. Various substances have been found which have proved their suitability for the investigation of regular binary eutectic growth [2–6]. However, very few substances have been reported that showed a non-faceted/non-faceted (nf/nf) peritectic reaction in a temperature range suitable for direct observation in a Bridgman furnace set-up. Barrio et al. [1] reported a peritectic reaction for the organic model alloy NPG (neopentylglycol)–TRIS (tris(hydroxymethyl)aminomethane). Both substances show an orientationally disordered crystalline phase at high temperature, generally called the “plastic phase”. This fact should permit the optical investigation of nf/nf peritectic solidification which is still not available to date. The reported phase diagram was constructed from differential scanning calorimetry (DSC) measurements and the evaluation of lattice parameters measured with X-ray diffraction [1].

The major aim of this work is to define the framework for in situ observations of oscillatory growth modes for peritectic alloys near the limit of constitutional undercooling. Due to the extremely small solidifi-

cation rates, the necessary observation time for such phenomena may take hours. Trivedi et al. presented experimental evidence for band structure formation during directional peritectic solidification in metals. These experiments required several hours for the formation of the alternating bands [7–10]. The macromolecules in organic model substances, that show metal-like solidification behaviour act in the same way as metal atoms do. However, the organic substance TRIS tends to decompose at temperatures above the melting point [11]. Therefore, the thermal stability of the corresponding model substances is of utmost importance.

The current work presents investigations on the thermal stability of the NPG–TRIS system obtained by DSC measurements and optical investigations of the solid/liquid interface held at a constant temperature gradient.

The organic substances NPG and TRIS were obtained from Aldrich [12] with an indicated purity of 99% and 99.9+%, respectively. Both compounds are reported to be highly hygroscopic [13]. In accordance with the material preparation published in Ref. [1], the water content of NPG was reduced, keeping the material in a dry atmosphere at 310 K for 24 h, whereas TRIS was used as delivered. Different types of sample geometries, sealing substances and procedures were tested. Due to the relatively high hot zone temperature of 493 K, which is needed to investigate the solid/liquid interface of the entire phase diagram, all sealing materials such as UV hardening and silica-based glues started leaking after some hours. The best results were obtained using square capil-

* Corresponding author. Tel.: +43 3842 402 3104; fax: +43 3842 402 2204; e-mail: johann.mogeritsch@mu-leoben.at

lary tubes (200 μm inner diameter and 100 μm wall thickness [14]) with fused ends. As both organic substances show reactions with humid air in the liquid state, the sample preparation was performed in a glovebox filled with argon. The humidity within the glove box was reduced to below 10^4 ppm and the oxygen content below 2×10^3 ppm, estimated with a hygrometer and an air oxygen measuring device.

For the preparation of the different initial alloy compositions the pure substances were weighed and mixed in small glass containers which were then closed with plastic caps. Next, the glass container was heated on a hot plate until the organic powder melted, then it was shaken to improve the mixing and then slowly solidified (~ 1 h) on a slightly heated (~ 313 K) plate. This procedure led to a refining of the alloys because impurities with a boiling temperature lower than the organic powder (e.g. water) should have condensed on the cap of the glass container. A similar refining procedure of the hygroscopic NPG was reported by Barrio et al. [1]. Due to the lower melting temperature of NPG compared to TRIS and the consequently different vapour pressure, a shift of the final alloy to higher TRIS values as compared to the weighed composition may happen. However, a corresponding compositional shift was estimated to be less than 1 mol.%. When the alloy was fully solidified, the glass container was crushed and the waxen alloy was ground and filled into a new storage container. From this container small amounts of the alloy were taken to fill the DSC samples and the aforementioned glass capillary tubes.

For the filling, the capillary tubes were laid on a hot plate such that one side was on the plate and the other side protruded freely. Small amounts of the alloy were deposited on the hot plate next to the open side of the tube. As soon as the alloy melted, the liquid was dragged into the tube by capillary forces until it reached the colder side of the tube where it solidified. This procedure ensured that enough room for expansion due to melting (and heating) was left free. Next, the capillary was slowly dragged off the hot plate, allowing the inner material to solidify. Before both ends of the glass capillary tube were sealed by melting the glass with a resistance heater, the end that had been placed on the hot plate was first “flash-heated” in order to evaporate the organic compound at the very end of the tube. During the investigations in the Bridgman furnace, both sides of the capillary tubes were outside of the Bridgman furnace and so kept around room temperature, so that the solid alloy further sealed the liquid.

The Bridgman furnace consisted of a cold and a hot copper block with a distance that was variable between 4 and 10 mm. The hot zone block was heated to temperatures between 443 and 523 K using Peltier elements; the cold zone temperature was controlled by a water circuit and set to temperatures between 278 and 353 K. The temperatures on both sides were measured with Pt 100 temperature sensors placed inside the copper blocks and regulated independently with an accuracy of ± 0.1 °C. The temperature gradients were measured with a 25 μm NiCr–Ni thermocouple within a filled capillary sample. The measured gradients were linear within the adiabatic/observation zone and ranged from 6 to

16×10^3 K m^{-1} . The microscope was equipped with a CCD camera and self-developed software allowing the recording and storage of images and temperature data with a frame rate of up to 10 images per second. Furthermore, the software allowed the measurement of positions in the field of view.

For the thermal stability investigations the samples were put in the Bridgman furnace and remained immobile for several hours. Up to five capillaries with different concentrations could be processed simultaneously. The hot and cold zones of the Bridgman set-up were ramped up to the predefined temperatures. Directly after the heating up of the hot side, the material started to melt and after approximately 1 h a stable planar solid/liquid interface indicated that (i) a stable temperature gradient in the samples had developed, and (ii) the diffusion field in the liquid and solid near the interface had equilibrated [15,16].

For the DSC measurements, 5 mg of each alloy composition was filled into Al pans that were hermetically sealed within a glovebox. Next, these DSC samples were investigated using a Perkin-Elmer Diamond calorimeter equipped with Pyris7 software that had been calibrated with In and Zn [17]. A similar instrument had been used by Barrio et al. [1] and Witusiewicz et al. [2]. The scanning rate was the same as reported in Ref. [1], i.e. 2 K min^{-1} . The evaluation of the measured DSC curves was performed according to the procedure given in Refs. [17,18]. Due to the relatively small liquidus/solidus separation, the DSC measurements reveal only single peaks for the transitions from liquid to solid. Boettinger et al. [18] showed that for small freezing ranges the maximum peak temperature lies above the liquidus temperature with an error increasing as the freezing interval decreases. It can therefore be concluded that the true liquidus temperature lies between the lower temperature onset point and the maximum peak temperature. This is reflected in the error bar for the liquidus temperature. The solidus temperature was taken at the first deviation from the baseline of the DSC curve. For a solid-state transformation the first onset point was taken. Furthermore, the transition curves for the solid/solid transition often showed shoulders, indicating a superposition of multiple peaks. In this case the onset of the phase transition was taken from the lowest temperature peak. Due to the overlapping of the peaks the transition temperature of the next peak segment was approximated with a tangent from the top of the shoulder peak segment. In Figure 1a, DSC traces for the different regions of the peritectic phase diagram are presented. The solid/liquid transition generally showed a clearly distinguishable single peak. Therefore this transition was the best for a direct comparison with the phase diagram published by Barrio et al. [1]. Samples taken from the same alloying preparation showed a standard deviation of ± 0.4 K for the liquidus temperature and ± 0.8 K for the solidus temperature, for the presented data the error bars correspond to ± 2 K. Note that the liquidus temperature can also be estimated during the optical investigation (see below) and can accordingly be taken for the assessment of the initial alloy composition.

The DSC measurements presented in Figure 1a indicate a peritectic plateau ranging from 47 to 64 mol.% NPG with clearly distinguishable single solid/solid and

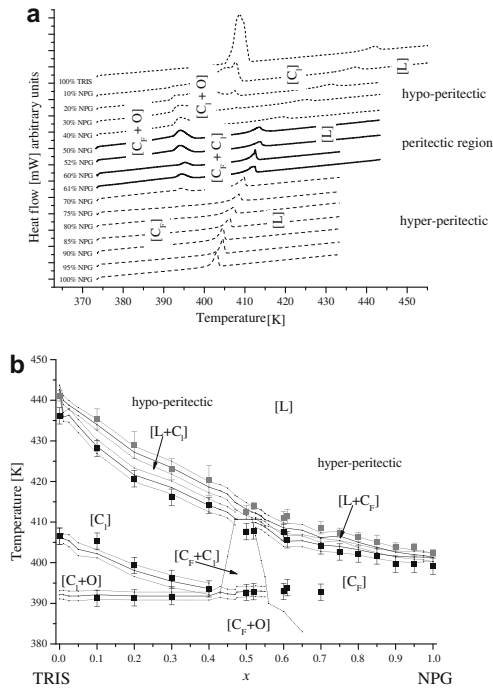


Figure 1. (a) DSC heating curves obtained with various alloy compositions and (b) phase diagram derived from the DSC measurements (points with error bars). For comparison, the reported diagram from Ref. [1] is also shown as straight lines with dotted error bands.

solid/liquid transition peaks. Compositions ranging from 0 to 48 mol.% NPG showed overlapping peaks for the solid/solid transition and detached solid/liquid transition peaks. The compositions from 65 to 100 mol.% NPG showed no clearly distinguishable solid/solid transition but a clear solid/liquid transition peak. In Figure 1b the results of our DSC measurements are compared with the phase diagram published in Ref. [1]: good agreement is found, within the limits of experimental error.

Figure 2a shows images of gradually decreasing NPG–TRIS compositions ~2 h after the beginning of melting. For all presented compositions the same temperature gradient of $G = 14 \text{ K mm}^{-1}$ had been applied over a gap of 4 mm. The upper edge of the picture corresponds to the end of the hot copper block. Barrio et al. [1] reported that

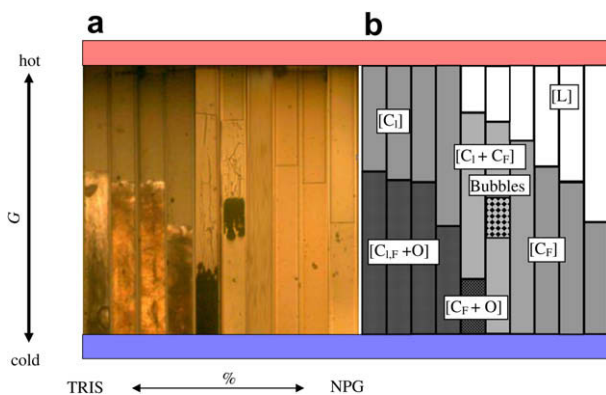


Figure 2. (a) “Optical phase diagram” with alloy compositions in approximately 10 mol.% steps; the samples stayed immobile in a stable temperature gradient around 2 h after melting; the temperature at the top of the picture is around 415 K and at the bottom around 380 K. (b) Corresponding interpretation of the different phases that occur.

the phase [O] is optically active, while the other two phases [C₁] and [C_F] are optically inactive (plastic phases). The optically active solid phase [O] in the TRIS-rich compositions could be clearly distinguished from the inactive phases even without using the polarization filters. When illuminated with white light, the optically inactive phases [C₁] and [C_F] appeared in the Bridgman furnace in a light brown colour depending on the illumination intensity, while the optically active phase [O] appeared as short coloured strands or simply dark brown or black. It was not possible to distinguish between the two optically inactive phases [C₁] and [C_F].

The sketch in Figure 2b represents the interpretation of the apparent phases based on these considerations. The four samples on the left-hand side in Figure 2a represent the hypoperitectic area with pure TRIS and 10, 20 and 30 mol.% NPG. In this case the maximum temperature in the observation field was lower than the liquidus temperature of these alloy concentrations, and so only the solid phases [C₁], [C₁ + O] and [C_F + O] appeared in the observation field. The next two samples, with alloy concentrations of 50 and 52 mol.% NPG, represent the peritectic region and showed the liquid phase, the two optically inactive phases [C₁] and [C_F], and the optically active phase [O]. The sample with a concentration of 52 mol.% NPG shows a group of small bubbles within the plastic zone and the faceted phase [O] occurs 3 h after melting (1 h delayed). The last four samples with concentrations of 60, 85, 95 mol.% NPG and pure NPG represent the hyperperitectic region and showed the liquid phase and the plastic phase [C_F]. In all cases the solid/liquid transition showed a straight line normal to the temperature gradient. The phase transition from the faceted [x + O] mixture phase ($x = C_F$ or C_1) to the non-faceted plastic phases [C_F] and [C₁] also showed a straight line. With the linear temperature gradient the positions of these straight phase transition lines could be converted to the corresponding temperatures, whereby the melting point of pure NPG was used as the offset point.

The solid/solid interface of the four samples on the left-hand side in Figure 2a, with 5, 15, 20 and 30 mol.% NPG, stay at the same position in the Bridgman furnace for more than 9 h. Here, the solid/liquid interface is in the hot zone of the Bridgman furnace and thus not visible. The two samples in the peritectic region, with alloy concentrations of 50 and 52 mol.% NPG, and the last four samples in the hyperperitectic region, with the concentrations of 70, 80, 90 mol.% NPG and pure NPG, showed a shift in the solid/liquid interface from the hot zone toward the cold zone up to 100 μm within 9 h. This could be a possible consequence of decomposition. The interface shift appeared to be dependent on the hot zone temperature, and the experiment time.

In Figure 3 the results of the evaluation of the interface temperatures taken 2 h after applying the temperature gradient have been plotted as points within the phase diagram as published by Barrio et al. [1]. The points show no error bars because they correspond to single experiments with a systematic error (measurement error of the temperature and positions) smaller than the point size. Taking the measurement accuracy into account, the phase transition temperatures agreed with the phase diagram published by Barrio et al. [1]. Gener-

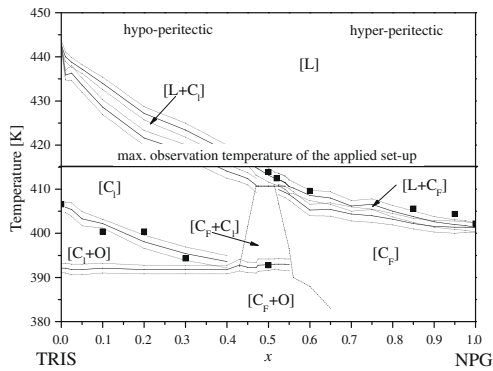


Figure 3. Comparison of the reported phase diagram [1] (lines with dotted error bands) with the optical investigations (points). The maximum temperature observable in the chosen Bridgman furnace is shown as a line at 415 K.

ally, the solid/solid transition is somewhat sluggish and therefore it takes some time until thermodynamic equilibrium is reached.

To establish the thermal stability of the macromolecules of the chosen materials, NPG and TRIS, separate DSC measurements have been performed where the pure materials and a representative alloy composition were exposed to an elevated temperature for several hours. For the thermal stability investigation, DSC measurement with a heating rate of 10 K min^{-1} was selected. Figure 4 summarizes the isothermal DSC measurements performed for pure NPG, pure TRIS and a 50% alloy composition, i.e. a peritectic alloy. The flat DSC lines for pure NPG (dotted lines in the graph) indicate that NPG was stable when exposed to temperatures up to 473 K, i.e. 10 K below the boiling point of NPG, for more than 4 h. The DSC curves for pure TRIS (continuous solid line) indicate that TRIS decomposed when exposed to a temperature of 473 K (i.e. 20 K below the boiling point) for more than 60 minutes. Upon reducing the exposure temperature to 463 and 453 K (10 K above its melting point) the stability time of TRIS gradually increased to 3 and more than 4 h, respectively. Further investigations on pure TRIS showed a thermal stability of more than 8 h when held at 438 K (curves not shown).

Furthermore, the DSC curves indicated decomposition after 3 h when exposed to a temperature of 473 K for the representative alloy composition of 50% NPG

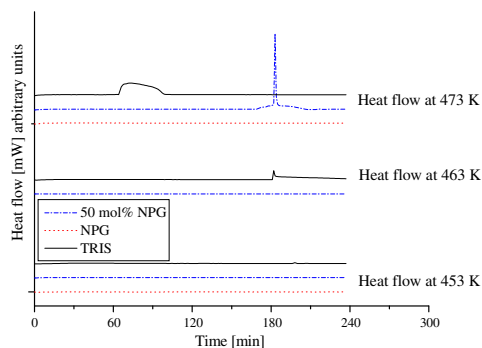


Figure 4. DSC traces of a peritectic alloy (50 mol.% NPG), dried “pure” NPG and as-delivered “pure” TRIS at different temperatures. The graph shows heat flow vs. time after having reached the selected annealing temperature.

(dash-dot line). However, no decomposition was found for 4 h at an exposure of 453 K. Therefore, it can be concluded that Bridgman-type optical investigations of the peritectic alloys NPG–TRIS should ideally be performed with a hot zone temperature around 450 K to enable sufficient experiment times (≥ 4 h).

NPG–TRIS shows a nf/nf peritectic phase diagram as reported by Barrio et al. [1]. Their reported DSC phase diagram could be confirmed within expected experimental errors.

- Optical investigations in a Bridgman set-up showed that the liquid phase can be clearly distinguished from the plastic solid phases. Furthermore, faceted and non-faceted solid phases could be observed. However, the two non-faceted phases $[C_F]$ and $[C_I]$ are both optically inactive, a fact that complicates a distinction between the two phases.
- Prolonged optical investigations showed a small shift of the solid/liquid interface toward lower temperatures within 9 h. This can be interpreted as a consequence of thermal decomposition.
- DSC isothermal annealing showed that NPG was stable for more than 4 h when held at temperatures up to 473 K. However, TRIS showed decomposition depending on the applied temperature. At 473 K, TRIS was stable for up to 90 min. A peritectic alloy of 50% NPG–TRIS was stable for 3 h at 473 K. At the hot zone temperature of 457 K all three samples were thermally stable for more than 4 h.

This work was funded by the European Space Agency (ESA) and the Austrian Space Agency (ASA) through means of the ESA MAP project METCOMP.

- [1] M. Barrio, D.O. Lopez, J. Ll. Tamarit, P. Negrier, Y. Haget, *J. Mater. Chem.* 5 (1995) 431.
- [2] V.T. Witusiewicz, L. Sturz, U. Hecht, S. Rex, *Acta Mater.* 52 (2004) 5519.
- [3] L. Sturz, V.T. Witusiewicz, U. Hecht, S. Rex, *J. Crystal Growth* 270 (2004) 273.
- [4] V.T. Witusiewicz, L. Sturz, U. Hecht, S. Rex, *Acta Mater.* 53 (2005) 173.
- [5] S. Akamatsu, G. Faivre, *Phys. Rev. E* 58 (1998) 3302.
- [6] S. Akamatsu, M. Plapp, G. Faivre, A. Karma, *Phys. Rev. E* 66 (2002) 0305011.
- [7] R. Trivedi, *Metall. Mater. Trans.* 26A (1995) 1583.
- [8] P. Mazumder, R. Trivedi, A. Karma, *Metall. Mater. Trans.* 31A (2000) 1231.
- [9] R. Trivedi, J.S. Park, *J. Cryst. Growth* 26A (2002) 572.
- [10] T.A. Lograsso, B.C. Fuh, R. Trivedi, *Metall. Mater. Trans.* 36A (2005) 1287.
- [11] R.E. Wasylshen, P.F. Barron, D.M. Doddrell, *Aust. J. Chem.* 32 (1979) 905–909.
- [12] <http://www.sigmaldrich.com>.
- [13] <http://fscimage.fishersci.com> search for 126-30-7 and 77-86-1.
- [14] <http://www.waleapparatus.com>.
- [15] M. Rettenmayr, M. Buchmann, *Mat. Sci. Forum* 508 (2006) 205.
- [16] H. Nguyen Thi, B. Drevet, J.M. Debierre, D. Camel, Y. Dabo, B. Billa, *J. Crystal Growth* 253 (2003) 539.
- [17] G.W.H. Höhne, W. Hemminger, H.-J. Flammerheim, *Differential Scanning Calorimetry*, Springer, Berlin, 1996.
- [18] W.J. Boettinger, U.R. Kattner, K.-W. Moon, J.H. Perepezko, *DTA and Heat-flux DSC Measurements of Alloy Melting and Freezing*, NIST Publication, 2006.